Proceedings of *The Riddle of Cooling Flows in Galaxies and Clusters of Galaxies*: E28
May 31 – June 4, 2003, Charlottesville, Virginia, USA
Ed. T. H. Reiprich, J. C. Kempner, & N. Soker

Observations of Central Radio Sources in Cooling Core Clusters

Tomislav Marković,[1,2] Frazer N. Owen,[1] and Jean A. Eilek [2]

[1] *National Radio Astronomy Observatory*
[2] *New Mexico Tech.*

We report preliminary results from a radio study of cluster center radio sources in cooling core clusters. Radio observations of a complete subset of 19 clusters have been performed using the VLA A and C arrays at 74 MHz, 327 MHz, and 1.4 GHz. We successfully detect radio emission from all cluster center sources, including two new detections in A1650 and A2142. All the extended sources have comparable physical and morphological properties to that of the well studied central radio source in M87. Our observations suggest that all cooling core clusters contain active radio galaxies in their cores, which we are seeing at different stages of their outburst, and that these radio sources could play important roles in the energetics of the cooling clusters cores.

1. Introduction

In dense central regions of cooling core clusters (CCC), the thermal intra-cluster medium (ICM) gas is observed to cool down to temperatures of $kT \sim 1$ keV (e.g. Peterson et al. 2003). This, however, is much warmer than the "cooling flow" model predicts. There has to be a physical mechanism which disables further cooling of the gas, thus preventing (or postponing) the CCC core collapse. In this paper, we look at cluster center radio sources (CCRS) as possible heating mechanisms to the cooling central regions. It is likely that many, if not all, cooling clusters contain active central radio galaxies, which play an important role in the dynamics of the local ICM. A few of these bright, nearby CCRS have been studied in detail. The latest images from the X-ray *Chandra* telescope show complex interactions between the radio source and the ICM (e.g. Blanton, Sarazin, & McNamara 2003). The holes in the X-ray emission are clearly coincident with the bubbles of the radio emission, indicating a displacement of the thermal gas by the relativistic particles of the radio jet. We also know that the CCRS can be energetically important—M87 in the Virgo cluster is one dramatic case. The energy carried by the M87 jet is at least as large as that radiated by the central regions of the ICM (Owen, Eilek, & Kassim 2000). Thus, it is suggestive that the CCRS could be capable of heating the cooling gas in some clusters.

This study applies an observational approach, utilizing primarily the VLA, to improve our understanding of the impact the CCRS have on the central regions of CCC. We try to answer whether the powerful CCRS, like the one in M87, are unusual or typical in their activity, and if all CCRS are currently active at any level. We search for signs of diffuse, extended emission emanating from the CCRS and study their spectra in order to see how their radio activity changes with time. A combination of frequencies and VLA arrays are used to accomplish the above. The low frequency (327 and 74 MHz) A array observations are performed in order to search for steep-spectrum emission which traces the older electron populations. These electrons, in turn, are signs of late stages of the CCRS outbursts. On the other hand, 20cm observations in C array are sensitive to flatter-spectrum, diffuse emission, and tell us about the current energization of cluster cores (as in M87). Ultimately, we try to answer whether all CCC contain radio galaxies which are strong enough, over time, to disrupt the gas cooling and provide the necessary pressure support. This is done so in combination with the theoretical work of Eilek (2004), also presented as a part of these proceedings.

Throughout this paper we assume the λCDM cosmology with $H_0 = 71$ km s^{-1} Mpc^{-1}.

2. The Cluster Sample and Radio Observations

We have formed a complete set of X-ray selected, nearby cooling core clusters for our radio observations. Such clusters can easily be distinguished from the general population by their centrally peaked surface brightness profiles, which can be well fit by the de Vaucoulers $r^{1/4}$ model (Eilek & Marković 2003). The ROSAT All-Sky Survey (RASS) includes a large number of candidate clusters, but the RASS images rarely justify the detailed deprojection analysis which is used to identify CCC. Instead, we select for high X-ray luminosity ($L_x > 3 \times 10^{43}$ erg/s within a 500 kpc aperture), and for a centrally peaked X-ray image; the latter is determined by visual inspection of images and by the ratio of flux within 62.5 kpc and 500 kpc apertures (from Ledlow et al. 2003). We also select by the presence of a dominant central galaxy coincident with X-ray peak. Applying these conditions to the RASS study of northern Abell clusters with $z < 0.09$ (Ledlow et al. 2003) gives us a complete subset of 22 clusters. There is an issue to be noted regarding our sample selection: the relatively small number of clusters in our sample is a result of a volume-limited survey—CCC are more common in the early flux-limited studies (such as Peres et al. 1998).

We used the Ledlow-Owen study (Ledlow & Owen 1995) and the NVSS (Condon et al. 1998) to identify radio sources associated with the central galaxy. All but two of the clusters had previously detected CCRS above

TABLE 1.

		327MHz								1.4GHz				
Cluster	z	Flux (mJy)	σ (mJy)	Power W Hz^{-1}	Size ($''$)	Size (kpc)	Spectral Index	Cluster	z	Flux (mJy)	σ (mJy)	Power W Hz^{-1}	Size ($''$)	Size (kpc)
A1644	0.0473	43	0.9	1.8E23	5.8x4.4	5.0x4.0	-0.57	A133	0.0566	164	0.04	1.0E24	100x70	110x80
A1650	0.0845	59	0.5	8.0E23	60x40	100x60		A193	0.0498	57	0.04	2.7E23	80x20	77x18
A1651	0.0846	18	0.5	2.4E23	4.5x3.5	7.0x5.0	0.76	A496	0.0327	134	0.05	2.7E23	45x30	30x20
A1688	0.0649	458	0.6	3.7E24	60x40	75x50	1.22	A2428	0.0833	12	0.03	1.6E23	120x60	185x90
A1795	0.0622	3215	1.9	2.4E25	45x30	55x35	0.86	A2495	0.0768	16	0.03	1.8E23	5x3	7.0x4.5
A1927	0.0740	37	0.6	3.8E23	4.5x3.0	6.0x4.0	0.97	A2597	0.0852	1893	0.11	2.6E25	4x2	6.0x3.5
A2029	0.0767	3660	0.7	4.1E25	60x45	85x65	1.33	A2626	0.0569	55	0.03	3.4E23	120x90	130x100
A2052	0.0348	30965	1.0	7.4E25	90x60	60x40	1.19	A2670	0.0759	7	0.03	7.7E22	13x1	18x1.5
A2063	0.0355	46	0.7	1.1E23	30x15	20x10	0.77							
A2142	0.0896	3.2	0.7	5.0E22	<7	<10								
A2199	0.0299	23148	1.0	3.9E25	120x60	70x35	1.26							

NOTE. — Columns (3) and (9) show total flux. Spectral index between 327 MHz and 1.4 GHz (NVSS). For tailed sources the angular length is the sum of two tails combined.

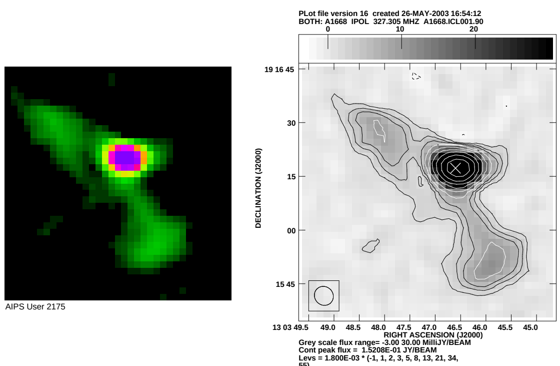

FIG. 1.— VLA A array image of A1668 at 327MHz and radio flux contour plot. The resolution is 6$''$. The cross is the optical position of the BCG.

2.5 mJy at 1.4 GHz. There was sufficient archive radio data for three of the clusters (A85, A426, and A780), so we observed the remaining 19 clusters in either VLA A or C arrays. The complete sample was split into two related observations in order to accommodate TM who hopes to finish his Ph.D. before the complete sample could be observed (at night) in both A and C arrays. We will complete the observations of the entire cluster set in both arrays at a later date.

Using the VLA A array, we observed eleven clusters at 90cm and 400cm (327 and 74 MHz). This was done simultaneously in 4P mode, since each of the wavelengths required only one IF. We observed in spectral line mode with total bandwidths of 6.25 MHz and 1.56 MHz, respectively for two wavelengths. At 90cm, the 3 hours of observations per cluster resulted in an rms of 0.5–1.0 mJy for all but one source, while the preliminary results at 400cm gave rms levels of 50–70 mJy. The linear resolution achieved at 90 cm was $\sim$5 kpc, with the lowest detected total radio luminosity of $\sim 0.5 \times 10^{23}$ W Hz^{-1} (i.e. 3 mJy at $z = 0.09$). The expected resolution at 400cm was 15–45 kpc, with the total flux density detection limit of $\sim 2{\times}10^{24}$ W Hz^{-1} (this work is still in progress).

The remaining eight clusters were observed in the VLA C array at 20cm (1.4 GHz). We used the pseudo-continuum "4" mode with 4×7×3.125 MHz channels in order to minimize the closure errors and achieve higher dynamic ranges. Each cluster was observed for 3 hours, enabling us to reach the rms of 30–40 μJy for the majority of sources, with the total flux detection limit of $\sim 3 \times 10^{21}$ W Hz^{-1}.

All the observations in both arrays were performed at night to minimize solar interference. The data was imaged using the AIPS program IMAGR, and self-calibrated using CALIB.

3. Results

3.1. *327 MHz and 1.4 GHz Data*

We have successfully detected all the CCRS at 327 MHz and 1.4 GHz, and list the relevant data in Table 1. The new, previously undetected sources are A1650 and A2142 (at 4σ level), with A1650 exhibiting significant, extended faint structure. This evidence supports the idea that all CCC have active radio sources in their cores. It also suggest that the CCRS are active at certain levels at all times.

All the extended sources, at 327 MHz and 1.4 GHz, exhibit additional faint emission around previously known jets and halos. The most striking example is that of A1668, shown in Figure 1. The 327 MHz data reveal previously undetected, extended, jet-like emission around the CCRS, which in many ways resembles the one in the familiar A2029 cluster (Figure 2).

Another interesting source is the single-lobed CCRS in A133, presented in Figure 3 (at 1.4GHz). It is likely that the two sources to the South, and one to the West of the bright central galaxy (BCG, marked with "x" in the image) are background sources. However, the lobe to the North appears connected to the central source on scales larger than the resolution of the image. The lobe has no optical counterpart, and has been classified as a radio relic (Slee et al. 2001). Fujita et al. (2002) have argued

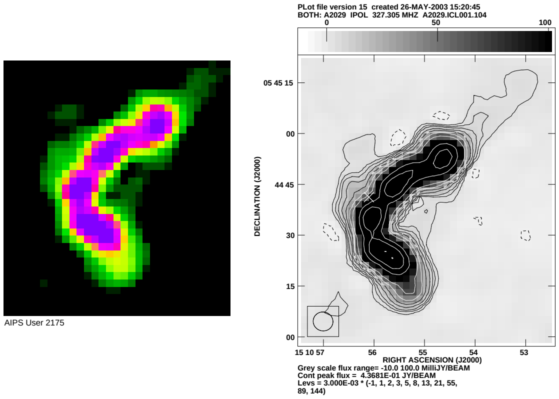

FIG. 2.— VLA A array image of A2029 at 327MHz and radio flux contour plot. The resolution is 6″. The cross is the optical position of the BCG.

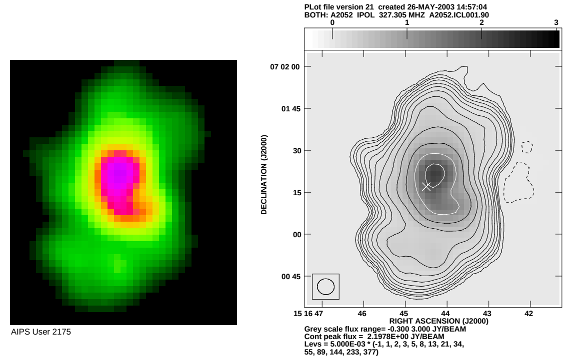

FIG. 4.— VLA A-array image of A2052 at 327MHz, and the radio flux contour plot. The resolution is 6 asec. The cross is the optical position of the BCG.

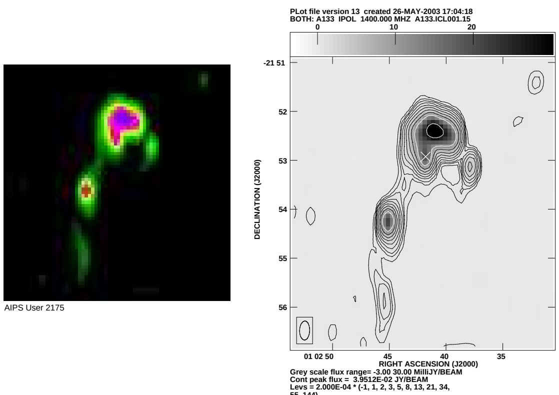

FIG. 3.— VLA C-array image of A133 at 1.4GHz, and the radio flux contour plot. The resolution is 15 asec. The cross is the optical position of the BCG.

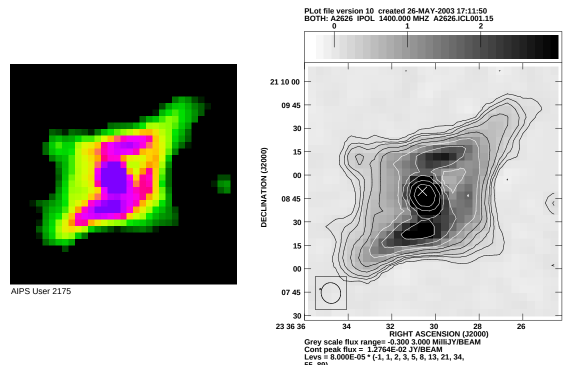

FIG. 5.— VLA C-array image of A2626 at 1.4GHz, and the radio flux contour plot. The resolution is 15 asec. The cross is the optical position of the BCG.

that the lobe had been detached from the cD galaxy, through buoyancy of the lobe or the motion of the host galaxy, while Rizza et al. (2000) have suggested the radio structure had been due to the interactions between the cD radio jet and the ICM. Our image supports the latter theory—the jet appears attached to the CCRS and is still strongly interacting with the ICM. The X-ray gas is being displaced by the CCRS emission, as suggested by Fujita et al. (2002), and seen in their *Chandra* images.

The amorphous, bubble-like radio halos are best seen in A2052 and A2626 (Figures 4 and 5, respectively). Their morphological properties (especially that of A2052), radio power, and linear extent resemble those of M87 (see Owen, Eilek, & Kassim 2000, or Eilek 2004). In the 327 MHz image of A2052, the CCRS (3C 317) is only slightly more extended than at 1.4 GHz (see Zhao et al. 1993). It seems that here, just like in M87, we see a clear edge to the radio bubble. This enables us to have a clearer picture of the linear scales at which certain bright CCRS influence the ICM, and possibly provides us with the information about the amount of their energy input to the central clusters' regions (see Eilek 2004 for more details).

Very similar conclusions can be drawn from the 1.4 GHz image of A2626. The longer exposure time has provided us with a much improved image when compared to Owen & Ledlow (1997) or Rizza et al. (2000). What previously seemed like several independent emission peaks is now clearly seen as a large radio bubble, fueled by two North-south oriented jets. As in M87, the jets are severely disrupted by the dense ambient medium, thus forming the amorphous structure observed. Future observations at 327 MHz should tell us if we are actually seeing the edge of the emission in this source.

The data for the sources which have not been discussed in detail are listed in Table 1. These sources will be fully analyzed, once the 74 MHz data reduction is completed, in Marković, Owen, & Eilek (2004).

3.2. *74 MHz Data*

Three clusters have been imaged thus far at 74 MHz—A1644, A2029, and A2052. The results are summarized in Table 2. We have not detected any emission above the 3σ level in A1644. This source is peculiar in nature. It has an inverted spectrum between 327 MHz and 1.4 GHz (see Table 1), and a non-detection here is not surprising. It may be an interesting source to study separately at different frequencies.

The 74 MHz images of the CCRS in A2029 and A2052 are presented in Figure 6. The Gaussian fit to A2052 gives the same angular scale as the one to 327 MHz data,

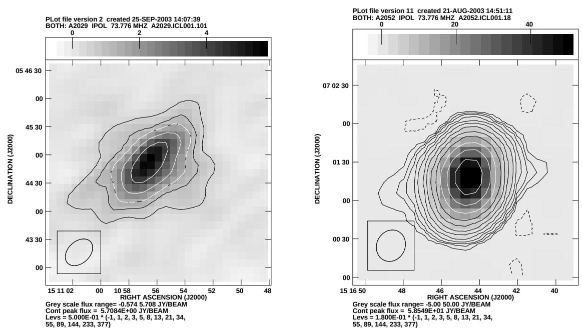

FIG. 6.— Contour images of A2029 (left) and A2052 (right) at 74 MHz.

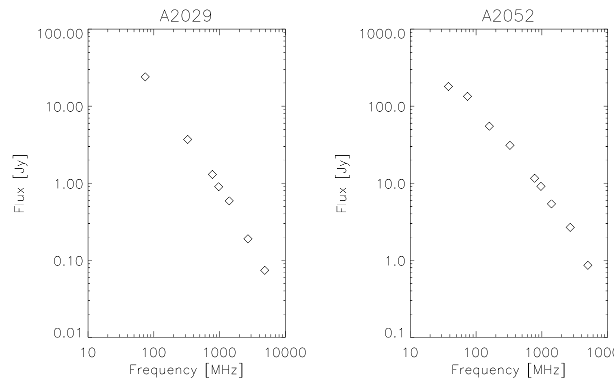

FIG. 7.— Spectral data for A2029 (left) and A2052 (right). The 74 and 327 MHz points from this study, others from CATS online catalog of radio sources (Verkhodanov, Trushkin, & Chernenkov 1997).

TABLE 2. 74 MHz DATA

74 MHz Cluster	Flux (mJy)	σ (mJy)	Power WHz^{-1}	Size ($''$)	Size (kpc)	Spectral Index
A1644	<200		<8.5E23			
A2029	24010	80	2.7E26	67x41	95x60	1.26
A2052	134120	60	3.1E26	90x60	60x40	1.00

NOTE. — Spectral index between 74 MHz and 327 MHz.

while its spectrum is almost as steep as at higher frequencies. This result seems to confirm that we are seeing all of the diffuse radio source in its spatial extent, and that the CCRS has a significant older electron population.

On the other hand, the 74 MHz image of A2029 shows appears more extended than the one at 327 MHz (Figure 2). It seems that this source contains a faint, diffuse radio bubble around its luminous jets. In order to test our sensitive imaging procedure, we have self-calibrated the 74 MHz UV data set with the 327 MHz image. The result has remained the same—we believe that the diffuse emission is real. This suggests that other jet-like CCRS could have faint halos around them, and that it is just a matter of having sensitive enough instrumentation to be able to detect them.

3.3. *Radio Spectra*

The radio spectrum of a source can be approximated by a power-law of the form

$$P_\nu \propto \nu^{-s}, \tag{1}$$

where s is defined as a spectral index of a radio source. With the exception of the peculiar A1664 source, all the CCRS studied thus far at lower frequencies (327 and 74 MHz) have steeper spectra than ordinary cluster radio sources (data in Tables 1 and 2). We also find that more powerful, extended CCRS tend to have steeper spectral indexes ($s \geq 1$) than the weaker ones ($s \leq 1$), and they also preferentially reside in clusters with denser X-ray cores (A2029, A2052, A2199 vs. A1651, A1927, A2063, but there are exceptions). This result, however, needs to be reinforced by a more detailed spectral studies of the CCRS observed only at 1.4 GHz.

The spectra of A2029 and A2052 are shown in Figure 7, with 74 and 327 MHz data points being from this study. Our data is in agreement with other spectral measurements—both of these sources have spectral indexes between $\alpha \sim 1.0$–1.5 across a range of frequencies. These signs of faster synchrotron aging, and older electron populations, may be caused by the presence of stronger magnetic fields in the cores of CCC.

4. **Discussion**

We are using an observational approach to study the role of CCRS in cooling clusters. Radio observations and imaging of 22 sources are being performed at 74 MHz, 327 MHz, and 1.4 GHz. In all the clusters we have successfully detected CCRS emission, including two previously undetected sources—A1650 and A2142. These facts suggest that all CCC are likely to host always active radio galaxies in their cores, and that we are observing them at different stages of their outburst.

The radio power of the CCRS should change over time, due to the ongoing energy input and electron synchrotron aging. It is rather natural, then, that our set contains both steeper and flatter-spectrum sources. The flatter spectrum CCRS could be going through the early stages in their activity, where the jets are just starting to energize the radio bubble, while the steeper spectrum ones are quieting down and are dominated by older electron populations.

We also find that the powerful radio galaxy M87 (Virgo cluster) is not unique in its properties. The majority of the extended sources in our sample exhibit radio emission on similar scales ranging from 30–100 kpc. Some of them are either close enough or bright enough that we are able to detect diffuse, bubble-like halos around their powerful radio jets. They also have comparable spectral indices and radio power to that of M87 (see comparison in Table 3). Since M87's heating power is comparable to the bremsstrahlung losses of the Virgo cluster cooling regions, it is likely that all of our extended CCRS are energetically important in their host clusters.

We are just starting to understand the role CCRS play in cooling clusters. We know they are different from other cluster radio galaxies—they have steeper spectra, are

Table 3. Comparison of M87 and several CCRS from our sample

Cluster	$P_{1.4GHz}$ (ergs/s)	Size 20cm (kpc)	Size 90cm (kpc)	Spectral Index
M87	1.7E40	40x30	40x30	0.8
A133	1.4E40	110x80		1.9
A193	3.8E39	77x18		
A496	3.8E39	30x20		0.2
A1688	8.7E39	≤ 5	75x50	1.22
A1795	9.5E40	40x15	55x35	0.86
A2029	8.3E40	50x20	85x65	1.33
A2052	1.8E41	40x35	60x40	1.19
A2199	1.3E41	45x20	70x35	1.26
A2626	8.8E40	130x100		1.4

Note. — Spectral index for sources observed only at 20cm from literature. M87 data from Owen, Eilek, & Kassim (2000).

smaller, and are morphologically more disturbed. These features are results of dense cluster center environments and stronger magnetic fields. Both radio, and X-ray data show clear interactions between the CCRS and the local ICM. In addition, we know that the radio outbursts are short lived when compared to cluster ages, so they would need to be repetitive in order to maintain the balance between the cooling and heating of the ICM.

Unfortunately, there are two important issues that remain less apparent. One of them is the triggering mechanism behind the radio outbursts. It is convenient to assume that the loss of pressure support in the densest cluster regions somehow awakens the CCRS so they can, in turn, heat up the cooling gas. These processes could keep recurring and indefinitely preventing the cluster core collapse. This scenario, however, does not fit in the picture of all other radio galaxies in clusters—the gas around them is not nearly as dense, and yet they can be as powerful as the CCRS. It is more likely that the CCRS emission is triggered by the events in the vicinity of the host galaxy black hole, on scales which are much smaller than the debated cooling regions. If this were true, the CCRS can be only a temporary solution to the cooling catastrophe.

An even more important question is if the CCRS alone are enough to offset cooling. We can calculate the total power stored in the ejected electrons and integrate it over all radio frequencies (as observed at present times), but those give us only a fraction of the answer. One needs to be able to estimate the CCRS input throughout their lifetime. Eilek (2004) finds that even then there might not be enough energy stored in the relativistic electrons alone. On the other hand, strong ion and magnetic field components might make the CCRS jets powerful enough to offset the radiation losses in most clusters, while the electron emission observed can primarily be used as a tracer of these more influential components. The CCRS can definitely have an impact, but we are not sure yet if they can be sufficient or permanent solutions to the "cooling flow" puzzle.

References

Blanton, E. L., Sarazin, C. L., & McNamara, B. R. 2003, ApJ, 585, 227

Condon, J. J., Cotton, W. D., Greisen, E. W., Yin, Q. F., Perley, R. A., Taylor, G. B., & Broderick, J. J. 1998, AJ, 115, 1693

Eilek, J. A. 2004, in "The Riddle of Cooling Flows in Galaxies and Clusters of Galaxies," ed. T. H. Reiprich, J. C. Kempner, & N. Soker (these proceedings)

Eilek, J. A. & Marković, T. 2003, in preparation.

Fujita, Y., Sarazin, C. L., Kempner, J. C., Rudnick, L., Slee, O. B., Roy, A. L., Andernach, H., Vikhlinin, & Ehle, M. 2002, ApJ, 575, 764

Ledlow, M. J. & Owen, F. N. 1996, AJ, 109, 853

Ledlow, M. J., Voges, W., Owen, F. N., & Burns, J. O. 2003, AJ, in press

Markovic, T., Owen, F. N., & Eilek, J. A. 2004, in preparation

Owen, F. N. & Ledlow, M. J. 1997, ApJS, 108, 41

Owen, F. N., Eilek, J. A., & Kassim, N. E. 2000, ApJ, 543, 611

Peres, C. B., Fabian, A. C., Edge, A. C., Allen, S. W., Johnstone, R. M., & White, D. A. 1998, MNRAS, 298, 416

Peterson, J. R., Kahn, S. M., Paerels, F. B. S., Kaastra, J. S., Tamura, T., Bleeker, J. A. M., Ferrigno, C., & Jernogan, J. G. 2004, in "The Riddle of Cooling Flows in Galaxies and Clusters of Galaxies," ed. T. H. Reiprich, J. C. Kempner, & N. Soker (these proceedings)

Rizza, E., Loken, C., Bliton, M., Roettiger, K., Burns, J. O., & Owen, F. N. 2000, AJ, 119, 21

Slee, O. B., Roy, A. L., Murgia, M., Andernach, H., & Ehle, M. 2001, AJ, 122, 1172

Soker, N. 2003, MNRAS, 342, 463

Verkhodanov, O. V., Trushkin, S. A., & Chernenkov, V. N. 1997, Baltic Astronomy, 6, 2, 275

Zhao, J. H., Sumi, D. M., Burns, J. O., & Duric, N. 1997, ApJ, 416, 51